ISSN 2075-1133, Inorganic Materials: Applied Research, 2023, Vol. 14, No. 3, pp. 641–648. © Pleiades Publishing, Ltd., 2023.
Russian Text © The Author(s), 2022, published in Fizika i Khimiya Obrabotki Materialov, 2022, No. 1, pp. 16–26.

PLASMOCHEMICAL METHODS OF PRODUCTION AND TREATMENT OF MATERIALS

The Film Properties Obtained from Aniline by Plasma Deposition at Atmospheric Pressure

M. P. Danilaev[a,*], I. R. Vakhitov[b,c,], S. V. Drobyshev[a,***], I. V. Lounev[b,****], B. Z. Kamaliev[b,*****], S. A. Karandashov[a,******], V. A. Kuklin[a,b,*******], and M. S. Pudovkin[b,********]**

[a] *Kazan National Research Technical University named after A.N. Tupolev—KAI, Kazan, 420111 Russia*

[b] *Kazan Federal University, Kazan, 420008 Russia*

[c] *Institute of Physics, Center for Quantum Technology, Kazan, 420008 Russia*

**e-mail: danilaev@mail.ru*

***e-mail: warlordik_009@mail.ru*

****e-mail: seregak2005@yandex.ru*

*****e-mail: iskvakhitov@gmail.com*

******e-mail: Lounev75@mail.ru*

*******e-mail: Bulat1596@gmail.com*

********e-mail: iamkvova@gmail.com*

*********e-mail: jaz7778@list.ru*

Received May 17, 2021; revised September 28, 2021; accepted October 1, 2021

Abstract—The properties of polymer films obtained in plasma of barrier discharge at atmospheric pressure from aniline of amorphous form with simultaneous formation of carbon particles in the films were studied. The threshold of discharge energy density was established (~30 mJ/m), beginning from which a continuous film filled with agglomerates of carbon particles can be obtained. The structure of such films corresponds to the form typical of amorphous polymers. Carbon particles form agglomerates, the concentration of which weakly depends on the discharge energy density and constitutes ~$(4–7) \times 10^4$ 1/cm^2, which does not allow increasing the conductivity. It was shown that the main contribution to the conductivity of films obtained from aniline and filled with carbon particles is made by the value of their moisture saturation. It was found that the creep of the material decreases with growth of the energy density, and hardness increases. This is associated with the formation and growth of the number of crosslinks in the samples with an increase in the energy input. The absolute values of Martens hardness correspond to the lower boundary for polyaniline, which is due to the small molecular weight of the obtained polymer.

Keywords: atmospheric pressure barrier discharge, carbon particles, conductivity

DOI: 10.1134/S2075113323030103

INTRODUCTION

Modern methods of forming polyaniline (PANI) films are directed to increasing their conductivity with simultaneous provision of high strength characteristics such as abrasion resistance and tensile strength [1, 2], which is due to wide prospects of practical application of such films as antistatic transparent coatings of organic glasses (polycarbonate, polymethylmethacrylate), elements of organic electronics for solar batteries and light emitting devices [3, 4], gas identification sensors [5, 6], and humidity sensors [7, 8].

Three main approaches to increasing of the conductivity of PANI films are distinguished: increase in the internal conductivity realized because of self-conductivity of polymer molecules; increase in external conductivity owing to introduction of a conductive filler, and the combination of these two approaches [9, 10]. It was shown in [10] that protonation of PANI allows stabilizing the positive charge appearing in molecules during oxidation and providing high conductivity of ~1 – 10 S/cm. Filling of PANI with carbon particles makes it possible to eliminate the barrier between conducting molecules of the polymer and thereby increase its conductivity. For example, filling of PANI films with carbon nanotubes (MWCNT and SWCNT) during its formation in microwave plasma allows increasing the conductivity from 10^{-8} S/cm for unfilled PANI to ~1–10 S/cm when filled with nanotubes by 1.5 wt % [11]. At such a mass concentration, the value of the volume concentration of carbon nanotubes will constitute 100–1000 μm^{-3} under condition of their uniform distribution in the polymer film.

Accounting for the fact that the length of carbon nanotubes reaches ~1 μm and their orientation is equiprobable, at such a concentration, particles will contact each other, forming external conductivity of PANI film.

It is necessary to note that low adhesion of carbon particles to the polymer matrix leads to agglomeration of particles [12], which decreases their volume concentration, and as a result, the PANI conductivity decreases. In addition, in this case, on the boundary particle–polymer, caverns are often formed, which leads to deterioration of the mechanical properties of the polymer film [13]. In [14], an increase in adhesion of carbon nanoparticles to PANI was provided owing to chemical bonds between graphene particles and polyaniline molecules, which allowed providing high stability of the conductivity of protonated PANI films filled with carbon nanoparticles in conditions of an increased humidity (~90%) upon solving the problem of identification of CO_2 gas. Adhesion of carbon particles of the filler to PANI can also be increased through the formation of PANI film in gas discharge plasma with simultaneous formation of carbon particles in it, as proposed, for example, in [15]. Carbon particles obtained in this way, including nanosized ones, can be charged, which initiates not only the process of polymerization of aniline with the formation of PANI but also the processes similar to protonation of PANI molecules [7].

The aim of this work is to study the structure and properties of the film obtained from aniline in plasma of barrier gas discharge of atmospheric pressure with simultaneous formation of carbon particles in it.

SAMPLING METHOD

The formation of an aniline film with the simultaneous formation of carbon particles in it was carried out in an AC barrier corona discharge according to the procedure described in [15–17] on a glass slide (SP-7102 glass with thickness of 1 mm). The strength of electric field was regulated in the range ~6–12 kV/cm with the accuracy of ±0.5 kV/cm. The formation of PANI film occurred from aniline vapor in an argon atmosphere. The pressure in the discharge chamber was 1040 ± 5 GPa. After obtaining the film, it was held in vacuum at a pressure not greater than 10^{-1} Torr and temperature of 95 ± 5°C for 4 h with a further temperature decrease to 20–25°C for 20 h. In the experiments, four types of PANI film samples were obtained at the following values of energy density released in the volume of the charge channel (streamer): sample 1, 15–20 mJ/m; sample 2, 24–27 mJ/m; sample 3, 30 ± 2 mJ/m; sample 4, 45 ± 2 mJ/m.

The surface morphology of the films obtained from aniline in plasma were studied on a Carl Zeiss Merlin scanning electron microscope. A graphite film with a layer of ~10 ± 2 nm was deposited on the surface of the samples to drain the charge from the samples during their analysis.

The film profile was studied on a Bruker DektakXT™ profilometer (stylus radius of 12.5 μm) with an error not worse than 10 nm.

Transmission electron microscopy (TEM) was carried out on a Zeiss Libra 120 microscope with a built-in OMEGA filter under the following conditions: accelerating voltage, 120 kV; electron source, LaB6. The analysis of electron diffraction reflections was carried out according to the procedure given in [25–28]. Absorption spectra were obtained on a StellarNet EPP2000 Spectrometer with a resolution of 0.5 nm.

The dielectric properties of the film samples were studied by dielectric spectroscopy at direct current according to GOST R 50499-93 (IEC 93-80) and at alternating current using a Novocontrol BDS-80 dielectric spectrometer. The measurement error of specific conductivity did not exceed 10%. Measurements of specific conductivity on alternating current were carried out at a temperature of ~23 ± 2°C and an applied voltage of 0.5 ± 0.05 V.

The Martens microhardness was measured on a Shimadzu DUH-211S ultramicrotester according to ISO 14577-1 using a Berkovich indenter (triangular indenter with apex angle of 115°), in much the same way as in [38].

RESULTS AND DISCUSSION

Study of the Morphology of the Films by the Method of Electron Microscopy

The surface of the films obtained from aniline in plasma (Fig. 1) corresponds to the form characteristic of amorphous polymers in contrast to the granular film structure obtained by electrochemical deposition or vacuum spraying [5, 10].

Carbon particles forming in plasma create agglomerates, which are distributed fairly uniformly along the surface of the samples and have an average size of 4–6 μm. No significant dependence of the average size of the agglomerates on the level of energy density was found. The change in their concentration has a weak tendency to increase with growth of energy input to the discharge and is estimated by the value of (4–7) × 10^4 cm^{-2}. At such a concentration, carbon agglomerates do not come in contact and most likely should not influence the electrical conductivity of the film samples.

The relief profile of the films is shown in Fig. 2.

At energy densities lower than ~30 mJ/m, a non-continuous film is formed. With growth of energy density, the rate of film growth increases from ~1.2 ± 0.2 μm/min (for energy density of ~25 mJ/m) to ~3 ± 0.5 μm/min (for ~45 mJ/m); disparate regions begin to combine with the formation of a continuous

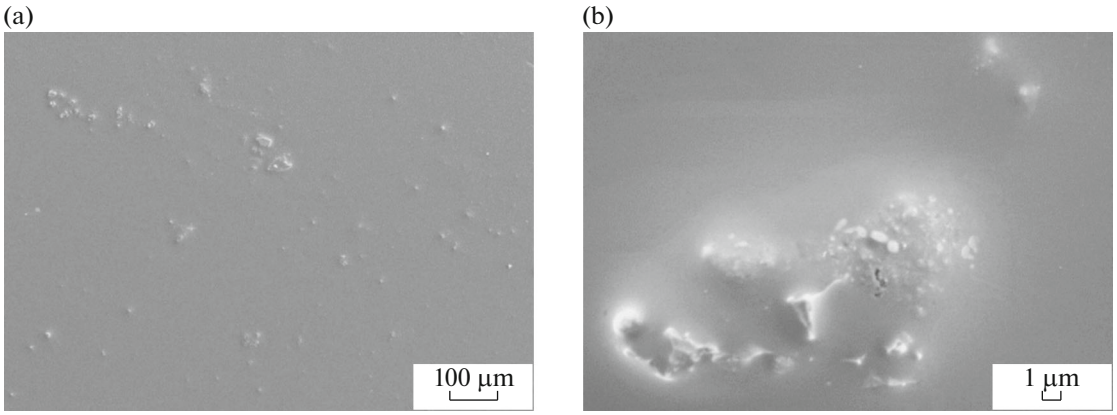

Fig. 1. Typical morphology of the film, sample 4.

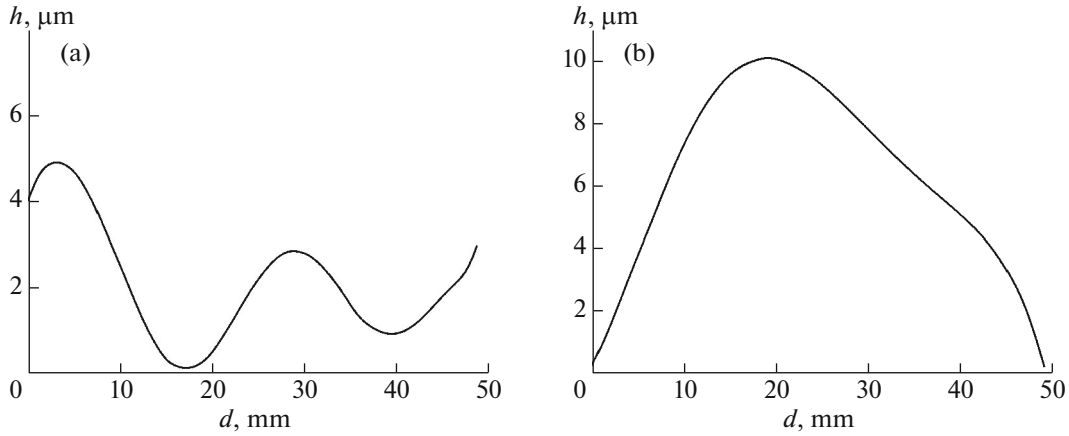

Fig. 2. Typical profiles of the film surface (*h*—height, *d*—width of films): (a) sample 1, (b) sample 3.

film. Beginning from the energy density of ~45 mJ/m, the growth rate of the polymer film constitutes ~3 ± 0.5 μm/min and weakly depends on further increase in energy density. This can be explained by concurrence of the processes of film formation and its destruction in gas discharge plasma [16] beginning from a specific energy density value in the discharge. It is necessary to note that destruction of aniline during the formation of the film leads to formation of both low molecular organic products and carbon particles, which influence the physicotechnical properties of the coating. In the case under consideration, an increase in discharge energy density, apparently, leads to an increase in the fraction of low molecular organic products in the film; an increase in the concentration of carbon particles with growth of energy density is not observed.

In this way, in the range of discharge energy densities of 15–27 mJ/m, a film with the least fraction of low molecular products is formed.

Absorption spectra (Fig. 3) of the film samples have characteristic peaks in the regions of 332, 420, 900, and 970 nm.

The absorption peak at a wavelength of 332 nm (Fig. 3a) corresponds to the benzene ring [14]. The absorption peak at $\lambda = 420$ nm is pronounced for samples 2–4 and is typical of protonated polyaniline (PANI) [14, 18]. It is known that PANI films have good moisture absorption [19]; therefore, after removing the film samples from the vacuum chamber into the atmosphere, the films were saturated with moisture, as evidenced by a weak peak in the region of 970 nm (Fig. 3b), which is characteristic of hydroxyl groups [20].

In the experiments, the humidity in the room was controlled by a hygrometer with an error of no more than 5%; its value was in the range of 75–85%. The presence of a significant amount of hydroxyl groups in the film contributed to the protonation of PANI films according to the mechanism described in [18]: a weak peak in the region of 900 nm is associated with the π-polaron [14, 21]. It should be noted that there are no peaks at 420, 980, and 900 nm in the transmission spectrum of sample 1. Perhaps this is due to the fact that, at the appropriate value of the energy density, the

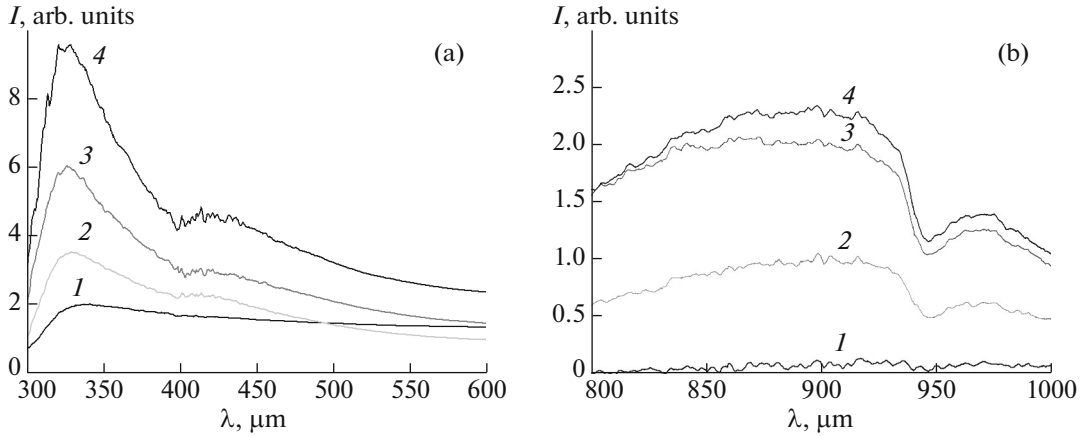

Fig. 3. Absorption spectra of the films: (*1–4*) samples 1–4, respectively.

formation of radicals necessary for the formation of PANI does not occur.

Identification of Allotropic Form of Carbon Particles by TEM Method

In a corona discharge, two regions are distinguished in which heat is released owing to the flow of electric current: these are the regions of ionization (corona sheath) and charge drift (streamers) [22, 23]. The plasma temperature in the corona sheath reaches ~4000°C for the operating modes of the experimental setup used [15, 23]. The average temperature of the medium in the volume of the streamer in the same modes is ~100–2200°C. At such temperatures, the destruction of aniline monomer macromolecules [24] and the formation of carbon particles of both amorphous and crystalline allotropic forms are possible.

For investigation of carbon particles by the TEM method (Fig. 4), a suspension was prepared by dissolving a polymer film in acetone (99.9%). After that, the obtained solution was held in an ultrasonic disperser for not less than 10 min (frequency of 44 kHz), the power of ultrasonic impact was ~10 W, and the solution was applied in the volume of 2 μL on a 3 mm copper gid with a Formvar/Carbon substrate (TedPella).

Diffraction analysis of the sample 3 showed a chaotic dislocation of reflections (Fig. 4f), which is due to agglomeration of carbon particles. Nevertheless, reflections corresponding to hexagonal structure in carbon particles can be distinguished in the obtained diffraction patterns, as well as in Fig. 4d: $d_{100}/d_{110} \approx 1.73$ [28].

The diffraction patterns of electrons (Fig. 4b) are close to those on multilayer carbon nanoparticles, for example, onion-like carbon [26, 28], and in Fig. 4f, on multilayer graphene structures (multilayered graphitic sheets) or soot crystallites [29, 30].

The results of TEM show the formation of both carbon particles with amorphous (Fig. 4b) and crystalline (Figs. 4d, 4f) allotropic forms. In this case, the fraction of particles with crystalline form increases with growth of energy input to the discharge, which is associated with the growth of temperature in the corresponding areas of the corona discharge.

Investigation of Dielectric Properties of the Films by the Method of Dielectric Spectroscopy

The main contribution to the conductivity of the obtained films from aniline in plasma is made by the value of their moisture saturation (Fig. 5). The volume concentration of carbon particles in the films is insufficient for increasing the external conductivity, and partial protonation with hydroxylic groups [20] does not allow increasing the conductivity. Reduction of the conductivity with an increase in the charge power is apparently associated with a decrease in the limiting moisture saturation of the film by means of formation of crosslinks between molecules and growth of the density of the polymer [31]. After drying of the film samples at pressure of ~10^{-1} Torr and temperature of ~23 ± 2°C, the conductivity was no greater than 10^{-8} S/cm.

It is necessary to note that, in a number of works, for example, [14, 32–34], the results of effective use of various sensors based on PANI films filled with carbon nanoparticles at an increased humidity of ~90% are presented.

Investigation of Mechanical Properties

The Martens microhardness was determined by the slope of the applied load increase curve and the change in the depth of the indenter impression at constant loading (C_{IT}, %—the parameter characterizing the creep of the material). Several independent measurements were carried out in different areas of the

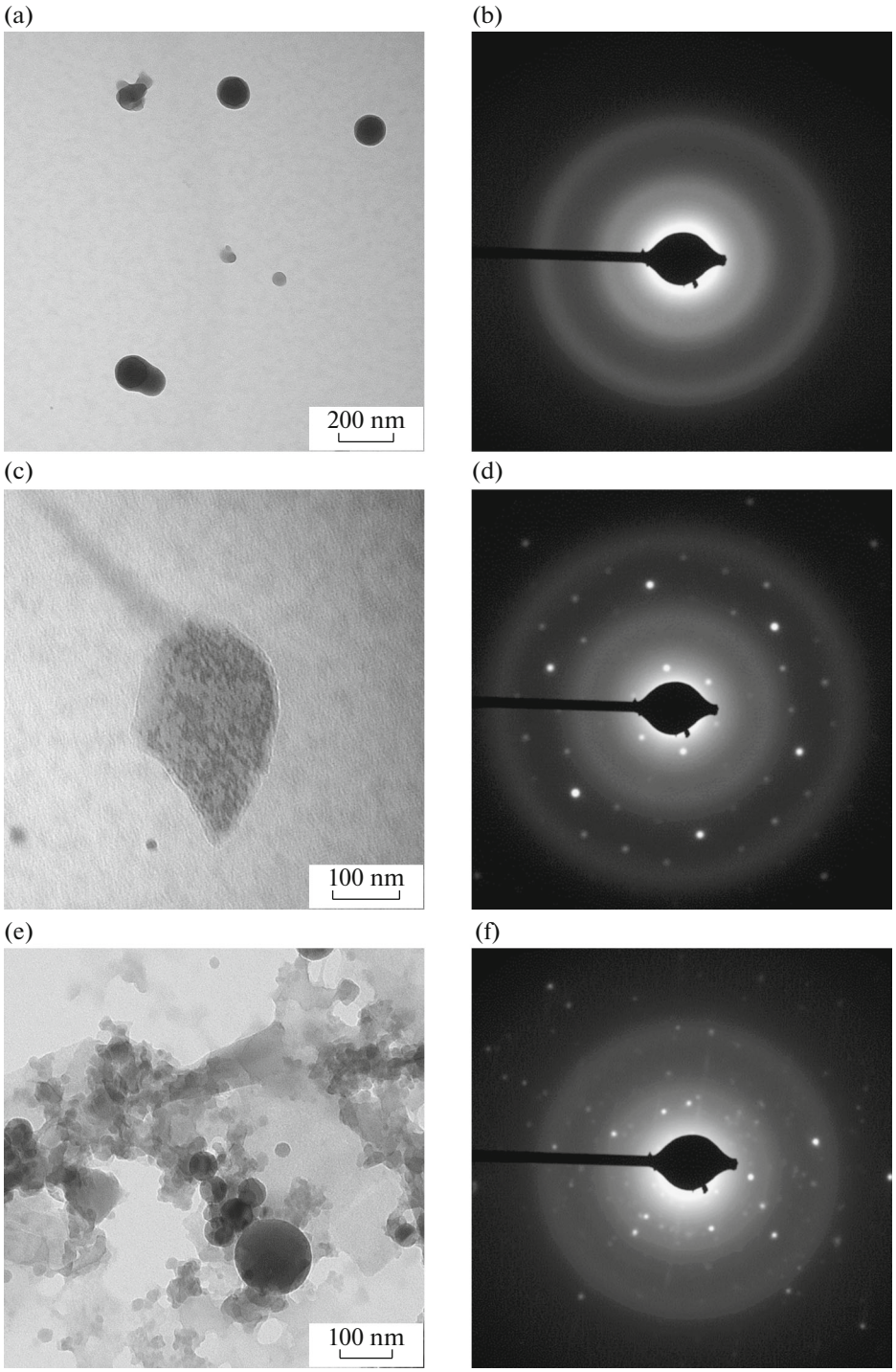

Fig. 4. Structures (a, c, e) and electron diffraction (b, d, f) of carbon particles obtained during the formation of PANI film (sample 3).

samples with further averaging of the obtained values (Table 1). The indenter indentation force was 0.17 mN; it was chosen in such a way as to minimize the influence of the substrate on the measurement results [38]; the exposure time at maximum load was 28 s; the parameter η_{IT} characterizes the elasticity of the material [36].

With growth of energy density, the creep of the material of the samples (C_{IT}) decreases somewhat, and the hardness increases. This may be caused by the for-

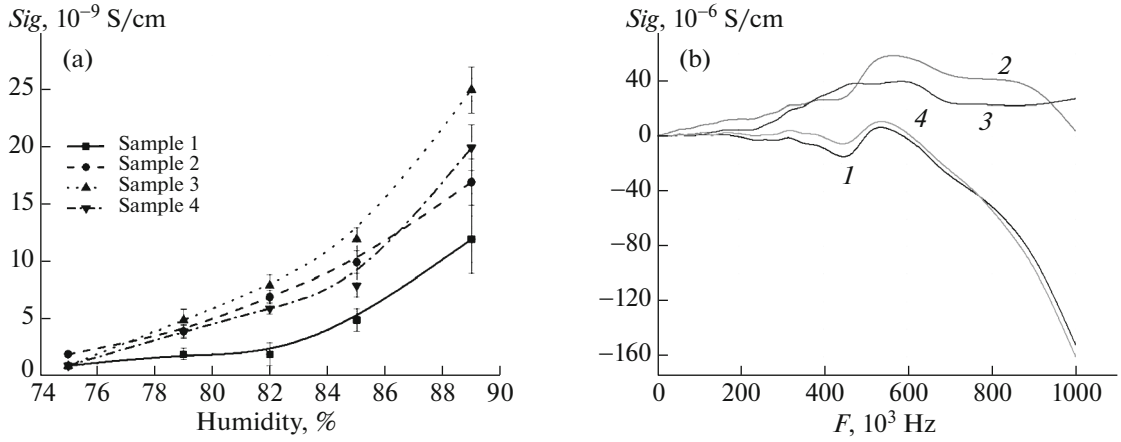

Fig. 5. (a) Dynamics of the conductivity of the films at direct current; (b) dielectric spectroscopy of sample 2 at humidity values: (*1*) 75%, (*2*) 89%, (*3*) 85%, (*4*) 79%.

mation and growth of the number of crosslinks in the samples with an increase in energy input [22, 37]. The absolute values of Martens hardness correspond to the lower boundary for polyaniline [38, 39], which is probably due to the small molecular weight of the obtained polymer.

CONCLUSIONS

The possibility of obtaining films from aniline of an amorphous form with simultaneous formation of carbon particles in them in the plasma of an AC barrier corona discharge at atmospheric pressure was experimentally confirmed.

The fraction of carbon particles of crystalline allotropic shape increases with growth of the discharge energy density, which is associated with an increase in temperature in the streamers and the corona discharge sheath. Carbon particles form agglomerates, the concentration of which weakly depends on the discharge energy density and constitutes ~$(4–7) \times 10^4$ cm^{-2}, which does not allow increasing the conductivity of the films by means of increasing the external conductivity.

Table 1. The results of measurements of the Martens microhardness

Sample	Martens hardness *HMs*, MPa	Material creep C_{IT}, %	Material elasticity η_{IT}, %
1	17.0 ± 0.5	38.6 ± 0.5	2.7 ± 0.2
2	17.5 ± 0.3	37.8 ± 0.3	2.8 ± 0.4
3	18.0 ± 0.4	37.2 ± 0.3	3.2 ± 0.3
4	18.6 ± 0.5	36.8 ± 0.3	3.0 ± 0.4

The main contribution to the conductivity of the films filled with carbon particles is made by their moisture saturation, which is determined by the structure of the coating and its continuity. It was established that the surface structure of the obtained films corresponds to the form characteristic of amorphous polymers. Continuity of the coating is achieved at energy densities higher than ~30 mJ/m, and the average rate of film growth changes from ~1.2 ± 0.2 μm/min (for energy density of ~25 mJ/m) to ~3 ± 0.5 μm/min (for ~45 mJ/m).

The microhardness of the films increases with growth of energy input to the discharge, which is due to the formation and growth of the number of crosslinks in the samples. The observed peaks in the regions of 420, 900, and 970 nm in the absorption spectra indicate the protonation of polyaniline films, which is initiated by hydroxyl groups according to the mechanism described in [20]. The corresponding peaks are observed only for continuous films, since at an energy density value of less than ~30 mJ/m, the formation of radicals necessary for the formation of PANI does not occur.

FUNDING

The scientific research (problem setting, development of experimental methods, analysis of the results obtained) was carried out with the financial support of the Ministry of Education and Science of the Russian Federation under agreement no. 1022041100774-3/1022041100496-8. Film profile studies were carried out at the expense of a subsidy allocated to the Kazan Federal University for the fulfillment of the state assignment in the field of scientific activity no. 0671-2020-0050 using the equipment of the Federal Collective Use Center of Physical and Chemical Research of Kazan Federal University.

REFERENCES

1. Nawaka, K. and Putson, C., Enhanced electric field induced strain in electrostrictive polyurethane composites fibers with polyaniline (emeraldine salt) spider-web network, *Compos. Sci. Technol.*, 2020, vol. 198, p. 108293. https://doi.org/10.1016/j.compscitech.2020.108293
2. Abutalib, M.M. and Rajeh, A., Preparation and characterization of polyaniline/sodium alginate-doped TiO_2 nanoparticles with promising mechanical and electrical properties and antimicrobial activity for food packaging application, *J. Mater. Sci.: Mater. Electron.*, 2020, vol. 31, no. 12, pp. 9430–9442.
3. Sankar, M.A., Surface functionalization of bio-inspired nanostructures in organic photovoltaics and electronics based on feathers of avian species for inherent UV and IR reflection, *Mater. Today: Proc.,* 2021, vol. 44, pp. 4576–4582. https://doi.org/10.1016/j.matpr.2020.10.823
4. *Halide Perovskites: Photovoltaics, Light Emitting Devices, and Beyond*, Sum, T.C. and Mathews, N., Eds., Wiley, 2019.
5. Mezhuev, Ya.O., Shtil'man, M.I., and Korshak, Yu.V., Application of polyaniline and polypyrrole in electronics, *Plast. Massy*, 2020, nos. 7–8, pp. 28–31.
6. Wang, R.-X., Huang, L.-F., and Tian, X.-Y., Understanding the protonation of polyaniline and polyaniline—graphene interaction, *J. Phys. Chem. C*, 2012, vol. 116, pp. 13120–13126.
7. Sandaruwan, C., Herath, H.M., Karunarathne, T.S., Ratnayake, S.P., Amaratunga, G.A., and Dissanayake, D.P., Polyaniline/palladium nanohybrids for moisture and hydrogen detection, *Chem. Cent. J.*, 2018, vol. 12, no. 1, p. 93. https://doi.org/10.1186/s13065-018-0461-y
8. Zhang, D., Wang, D., Li, P., Zhou, X., Zong, X., and Dong, G., Facile fabrication of high-performance QCM humidity sensor based on layer-by-layer self-assembled polyaniline/graphene oxide nanocomposite film, *Sens. Actuators, B*, 2018, vol. 255, pp. 1869–1877.
9. Boeva, Z.A. and Sergeyev, V.G., Polyaniline: Synthesis, properties, and application, *Polym. Sci., Ser. C,* 2014, vol. 56, no. 1, pp. 144–153. https://doi.org/10.1134/S1811238214010032
10. Kompan, M.E., Sapurina, I.Yu., Babayan, V., and Kazantseva, N.E., Electrically conductive polyaniline—A molecular magnet with the possibility of chemically controlling the magnetic properties, *Phys. Solid State*, 2012, vol. 54, no. 12, pp. 2400–2406. https://doi.org/10.1134/S1063783412120190
11. Ndiaye, A.A., Lacoste, A., Be's, A., Zaitsev, A., Poncin-Epaillard, F., and Debarnot, D., A better understanding of the very low-pressure plasma polymerization of aniline by optical emission spectroscopy analysis, *Plasma Chem. Plasma Process.*, 2018, vol. 38, no. 4, pp. 887–902.
12. Ashraf, M.A., Peng, W., Zare, Y., and Rhee, K.Y., Effects of size and aggregation/agglomeration of nanoparticles on the interfacial/interphase properties and tensile strength of polymer nanocomposites, *Nanoscale Res. Lett.*, 2018, vol. 13, no. 1, p. 214. https://doi.org/10.1186/s11671-018-2624-0
13. Chu, C., Ge, H., Gu, N., Zhang K., and Jin, C., Interfacial microstructure and mechanical properties of carbon fiber composite modified with carbon dot, *Compos. Sci. Technol.,* 2019, vol. 184, p. 107856. https://doi.org/10.1016/j.compscitech.2019.107856
14. Karouei, S.F.H., Moghaddam, H.M., and Niavol, S.S., Characterization and gas sensing properties of graphene/polyaniline nanocomposite with long-term stability under high humidity, *J. Mater. Sci.,* 2021, vol. 56, no. 6, pp. 4239–4253.
15. Danilaev, M.P., Bogoslov, E.A., Kuklin, V.A., Vakhitov, I.R., Kamaliev, B.Z., Lounev, I.V., Evtyugin, V.G., Rogov, A.M., Osin, Yu.N., and Tagirov, L.R., Single-stage plasma-chemical synthesis and characterization of carbon nanoparticle-polymer suspensions, *Plasma Processes Polym.*, 2020, vol. 17, no. 4, p. 1900204. https://doi.org/10.1002/ppap.201900204
16. Bogoslov, E.A., Danilaev, M.P., Polskii, Y.E., Vakhitov, I.R., Gumarov, A.I., Yanilkin, I.V., and Tagirov, L.R., Morphology of polymer film coatings produced in a barrier gas discharge at atmospheric pressure, *Inorg. Mater.: Appl. Res.,* 2018, vol. 9, no. 3, pp. 385–388.
17. Danilaev, M.P., Bogoslov, E.A., Polsky, Yu.E., Yanilkin, I.V., Vakhitov, I.R., Gumarov, A.I., and Tagirov, L.R., Internal stresses in plasma deposited polymer film coatings, *Inorg. Mater.: Appl. Res.*, 2019, vol. 10, no. 3, pp. 556–559.
18. Wang, J., Polyaniline coatings: Anionic membrane nature and bipolar structures for anticorrosion, *Synth. Met.,* 2002, vol. 132, no. 1, pp. 53–56.
19. Ghosh, P., Sarkar, A., Ghosh, M., et al., A study on Hall voltage and electrical resistivity of doped conducting polyaniline, *Czech. J. Phys.,* 2003, vol. 53, no. 12, pp. 1219–1227.
20. Zuev, V.E. and Krekov, G.M., *Sovremennye problemy atmosfernoi optiki, Tom 2: Opticheskie modeli atmosfery* (Modern Problems of Atmospheric Optics, vol. 2: Optical Models of the Atmosphere), Leningrad: Gidrometeoizdat, 1986.
21. Borah, R., Banerjee, S., and Kumar, A., Surface functionalization effects on structural, conformational, and optical properties of polyaniline nanofibers, *Synth. Met.*, 2014, vol. 197, pp. 225–232.
22. *Entsiklopediya nizkotemperaturnoi plazmy. Tom 2: Generatsiya plazmy i gazovye razryady. Diagnostika i metrologiya plazmennykh protsessov* (Encyclopedia of a Low-Temperature Plasma, vol. 2: Plasma Generation and Gas Discharges. Diagnostics and Metrology of Plasma Processes), Fortov, V.E., Ed., Moscow: Nauka, 2000.
23. Bogoslov, E.A., Danilaev, M.P., Drobyshev, S.V., and Kuklin, V.A., Semiemprical estimate of the temperature of the medium in the corona discharge of a plasma-chemical reactor, *J. Eng. Phys. Thermophys.,* 2020, vol. 93, no. 6, pp. 1591–1597.
24. Gurvich, L.V., Karachevtsev, G.V., Kondrat'ev, V.N., et al., *Energii razryva khimicheskikh svyazei. Potentsialy ionizatsii i srodstvo k elektronu* (Chemical Bond Breaking Energies. Potentials Ionization and Electron Affinity), Moscow: Nauka, 1974.

25. Hammond, C., *The Basic of Crystallography and Diffraction,* Oxford: Oxford Sci., 1997.
26. Hirahara, K., Bandow, S., Suenaga, K., Kato, H., Okazaki, T., Shinohara, H., and Iijima, S., Electron diffraction study of one-dimensional crystals of fullerenes, *Phys. Rev. B,* 2001, vol. 64, p. 115420.
27. Colomer, J.-F., Henrard, L., Launois, P., Van Tendeloo, G., Lucas, A.A., and Lambin, Ph., Interpretation of electron diffraction from carbon nanotube bundles presenting precise helicity, *Phys. Rev. B*, 2004, vol. 70, p. 075408.
28. Müller, U., *Symmetry Relationships between Crystal Structures: Applications of Crystallographic Group Theory in Crystal Chemistry*, Oxford: Oxford Univ. Press, 2013.
29. Feuerbacher, M., Heidelmann, M., and Carsten, Th., Hexagonal high-entropy alloys, *Mater. Res. Lett.*, 2014, vol. 3, no. 1, pp. 1–6.
30. Eletskii, A.V., Iskandarova, I.M., Knizhnik, A.A., and Krasikov, D.N., Graphene: Fabrication methods and thermophysical properties, *Phys.-Usp.*, 2011, vol. 54, pp. 227–258.
31. Cruz, G.J., Morales, J., Castillo-Ortega, M.M., and Olayo, R., Synthesis of polyaniline films by plasma polymerization, *Synth. Met.*, 1997, vol. 88, no. 3, pp. 213–218.
32. Liu, G., Zhou, Y., Zhu, X., et al., Humidity enhanced ammonia sensing of porous polyaniline/tungsten disulfide nanocomposite film, *Sens. Actuators, B*, 2020, vol. 323, pp. 1–14.
33. Liu, C., Tai, H., Zhang, P., Yuan, Z., Du, X., Xie, G., and Jiang, Y., A high-performance flexible gas sensor based on self-assembled PANI-CeO_2 nanocomposite thin film for trace-level NH_3 detection at room temperature, *Sens. Actuators, B*, 2018, vol. 261, pp. 587–597.
34. Manjunatha, S., Machappa, T., Ravikiran, Y.T., Chethan, B., and Sunilkumar, A., Polyaniline based stable humidity sensor operable at room temperature, *Phys. B*, 2019, vol. 561, pp. 170–178.
35. Jain, S., Chakane, S., Samui, A.B., Krishnamurthy, V.N., and Bhoraskar, S.V., Humidity sensing with weak acid-doped polyaniline and its composites, *Sens. Actuators, B*, 2003, vol. 96, nos. 1–2, pp. 124–129.
36. Detector, P.U.F., Ultra micro hardness testers measure surface strength properties, *Pract. Failure Anal.*, 2003, vol. 3, pp. 3–11.
37. Yasuda, H., *Plasma Polymerization*, Orlando, Florida: Academic, 1985.
38. Kang, E.T., Ma, Z.H., Tan, K.L., Tretinnikov, O.N., Uyama, Y., and Ikada, Y., Surface hardness of pristine and modified polyaniline films, *Langmuir*, 1999, vol. 15, no. 16, pp. 5389–5395.
39. Passeri, D., Alippi, A., Bettucci, A., Rossi, M., Tamburri, E., and Terranova, M.L., Indentation modulus and hardness of polyaniline thin films by atomic force microscopy, *Synth. Met.*, 2011, vol. 161, nos. 1–2, pp. 7–12.

Translated by K. Gumerov